

# Non-stationary filtered shot noise processes and applications to neuronal membranes

Marco Brigham, Alain Destexhe

December 7, 2024

## Abstract

Filtered shot noise processes have proven to be very effective in modelling the evolution of systems exposed to stochastic shot noise sources, and have been applied to a wide variety of fields ranging from electronics through biology. In particular, they can model the membrane potential  $V_m$  of neurons driven by stochastic input, where these filtered processes are able to capture the non-stationary characteristics of  $V_m$  fluctuations in response to pre-synaptic input with variable rate. In this paper, we apply the general framework of Poisson Point Processes transformations to analyse these systems in the general case of variable input rate. We obtain exact analytic expressions, and very accurate approximations, for the joint cumulants of filtered shot noise processes with multiplicative noise. These general results are then applied to a model of neuronal membranes subject to conductance shot noise with continuously variable rate of pre-synaptic spikes. We propose very effective approximations for the time evolution of  $V_m$  distribution and simple method to estimate the pre-synaptic rate from a small number of  $V_m$  traces. This work opens the perspective of obtaining analytic access to important statistical properties of conductance-based neuronal models such as the the first passage time.

## 1 Introduction

We investigate the statistical properties of systems that can be described by the filtering of shot noise input through a first-order Ordinary Differential Equation (ODE) with variable coefficients. Such systems give rise to filtered shot noise processes with multiplicative noise. The membrane potential  $V_m$  fluctuations of neurons can be modeled as filtered shot noise currents or conductances [1, 2]. These fluctuations have been previously analysed in the stationary limit of shot noise conductances with constant rate, and an exact analytical solution has been obtained for the mean and joint moments of exponential shot noise [3, 4]. However, many neuronal systems evolve in non-stationary regimes driven by shot noise with variable input rate. A typical example is provided by visual system neurons that receive pre-synaptic input with time-varying rate that reflects an evolving visual landscape. Modeling studies often consider the exponential shot noise case, whereas biological systems may display larger diversity including slow rising impulse response functions similar to the alpha and bi-exponential functions, for example. Previous studies have addressed non-stationary exponential shot noise conductances [5] and non-stationary currents [6].

Poisson Point Processes (PPP) provide a natural model of random input arrival times that are distributed according to a Poisson law that may vary in time. Application-oriented treatments of PPP theory and PPP transformations can be found in [7, 8]. The key idea of this article is to express the filtered process as a transformation of random input arrival times and to apply the properties of PPP transformations to derive its non-stationary statistics. Using this formalism we derive exact analytical expressions for the mean and joint cumulants of the filtered process in the general case of variable input rate. We develop an approximation based on a power expansion of the deterministic solution. We apply these results to a simple neuronal membrane model of sub-threshold membrane potential  $V_m$  fluctuations that evolves under shot noise conductance with continuously variable rate of pre-synaptic spikes.

Shot noise processes are simple yet powerful models of stochastic input that correspond to the superposition of impulse responses arriving at random times according to a Poisson law. Systems evolving under shot noise input have been observed across many domains, such as electronics [9, 10], optics [11, 12] and many other fields [13, 14]. Shot noise was discovered in the early works of Campbell and Schottky [9, 10]. Key theoretical results were obtained by Rice [15] and a modern review of their probabilistic structure is presented in [16]. Filtered shot noise processes with multiplicative noise are an extension of *Filtered Poisson Process* [8, 13, 14] that are generated by linear transformations of PPP.

In this article, we start by presenting a simple model of filtered shot noise process with multiplicative noise and variable input rate (Section 2). We next consider the general case of PPP transformations, whose properties are presented in Section 3, and exact analytic expressions for the joint cumulants of the filtered process are derived (Section 4), as well as an approximation of the exact analytical solution (Section 5). Finally, we apply these results to a simple neuronal membrane model of sub-threshold  $V_m$  fluctuations with continuously variable rate of pre-synaptic spikes (Section 6).

## 2 Model of Filtered Shot Noise Process

In this section we present a simple model of filtered shot noise process with multiplicative noise. This stochastic process results from the filtering of shot noise input through a first-order ODE with variable coefficients. We show that under very simple input rate conditions the filtered process is non-stationary. We derive the time course of the filtered process in terms of the shot noise arrival times. The simulation parameters are presented at the end of the section.

Consider the time evolution  $Y(t)$  of a system governed by a first-order ODE with variable coefficients that is driven by shot noise input  $Q(t)$ :

$$\tau \frac{d}{dt} Y(t) = -Y(t) + (1 - Y(t)) Q(t) \quad (1)$$

$$Q(t) = \sum_{x_j \in \xi} g(t - x_j) H(t - x_j) \quad (2)$$

where  $\tau$  is a time constant,  $\xi$  is the set of shot noise arrival times,  $g(t - x_j) H(t - x_j)$  is the impulse response function at time  $t$  for arrival time  $x_j \in \xi$  and  $H(u)$  is the Heaviside function. The impulse response function is also known as *shot noise kernel*.

The input arrival times  $\xi$  in Eq. (2) are distributed according to a Poisson law as is characteristic of shot noise. The time evolution of this system is both stochastic and deterministic: stochastic since it is driven by random input arrival times  $\xi$ , but also deterministic since there is a unique outcome for each  $\xi$ . The system response  $Y(t, \xi)$  is said to be a filtered version of the shot noise process  $Q(t, \xi)$  since it is described by the first-order ODE in Eq. (1).

We'll introduce non-stationary dynamics in our model by restricting the input arrival times to occur between  $t_a$  and  $t_b \geq t_a$  with a constant Poisson rate  $\lambda$ . One realization of shot noise input  $Q(t, \xi)$  and the resulting system response  $Y(t, \xi)$  are shown in Fig. 1. The mean and standard deviation ( $\mu \pm \sigma$ ) of both processes are clearly non-stationary since they vary in time.

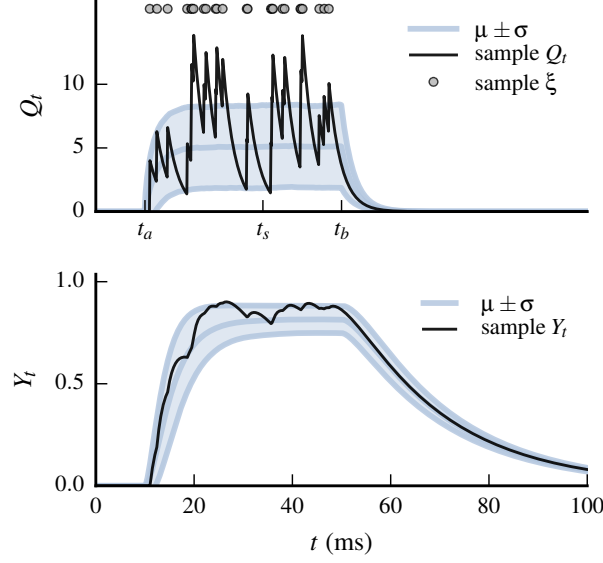


**Figure 1** – (color online) Single realization and basic statistics of filtered shot noise process  $Y_t$  under shot noise input  $Q_t$ . (Top) Random input arrival times  $x_j \in \xi$  generate non-stationary shot noise  $Q_t \equiv Q(t, \xi)$ . (Bottom) Non-stationary system response  $Y_t \equiv Y(t, \xi)$  driven by shot noise  $Q_t$ . The input arrival times are distributed with a variable Poisson rate  $\lambda(t)$  that restricts the arrivals to occur between  $t_a$  and  $t_b$ . A single realization of random arrival times  $\xi$  is represented by gray dots (top), realizations of  $Q_t$  and  $Y_t$  are shown in black. The mean and standard deviation ( $\mu \pm \sigma$ ) of  $Q_t$  and  $Y_t$  are shown in blue and are clearly non-stationary. The simulation parameters are detailed at the end of this section.

The system response  $Y(t, \xi)$  for a particular shot noise input  $Q(t, \xi)$  is obtained by solving Eq. (1). For a given set of input arrival times  $\xi$  and initial value  $Y_0 = 0$ ,

$$\begin{aligned} Y(t, \xi) &= \frac{1}{\tau} \int_{-\infty}^t e^{-\frac{t-z}{\tau}} Q(z, \xi) e^{-\frac{1}{\tau} \int_z^t Q(u, \xi) du} dz \\ &= \frac{1}{\tau} \int_{-\infty}^t e^{-\frac{t-z}{\tau}} \sum_{x_j \in \xi} g(z - x_j) H(z - x_j) \prod_{x_i \in \xi} e^{-\frac{1}{\tau} \int_z^t g(u - x_i) H(u - x_i) du} dz \end{aligned} \quad (3)$$

The input arrival times  $\xi$  completely determine the time evolution of  $Y(t, \xi)$ . The Eq. (3) also shows that the response at time  $t$  for each input arrival  $x_j$  also depends on later input arrivals  $x_j \leq x_i \leq t$ . For a single shot noise source the solution can be further simplified using integration by parts:

$$Y(t, \xi) = 1 - \frac{1}{\tau} \int_{-\infty}^t e^{-\frac{t-z}{\tau}} \prod_{x_i \in \xi} e^{-\frac{1}{\tau} \int_z^t g(u - x_i) H(u - x_i) du} dz \quad (4)$$

The remainder of this article addresses the question of how to obtain the cumulants of the quantity on the left side of Eq. (4) from those on the right side, in the particular case of Poisson distributed input arrival times  $\xi$  with variable rate  $\lambda(t)$ . For simplicity of exposure, we consider Eq. (4) instead of Eq. (3). While latter can be tackled with the *Slivnyak-Mecke Theorem* [17, 18] it would lead to a slightly more complex presentation.

The numerical simulations were generated with exponential shot noise kernel  $g(t - x) = h \exp(-(t - x)/\tau_s)$  and the rectangular-shaped rate function  $\lambda(t)$  that is represented in the upper half of Fig. 2. Other parameters are  $\tau = 0.02$  s,  $\lambda = 500$  Hz,  $h = 4\text{E-}9$  S and  $\tau_s = 0.0025$  s.

### 3 Causal Point Process Transformations

We review the basic properties of PPP transformations and analyze the stochastic process generated by causal PPP transformations. The expectation of PPP transformations yields the joint cumulants of the associated

processes. We illustrate this approach with the shot noise process and compare the predicted mean and second order cumulants with numerical simulations.

We consider a Poisson Point Process  $\Xi(\mathcal{S}, \lambda)$  that generates *points* in the interval  $\mathcal{S} \subseteq \mathbb{R}$  of the real line with rate function  $\lambda(x) \geq 0$  such that  $m(\mathcal{S}) \equiv \int_{\mathcal{S}} \lambda(x) dx$  is finite for any bounded interval  $\mathcal{S}$ . A realization  $\xi$  of  $\Xi$  contains the set of points  $\{x_1, \dots, x_n\} \in \mathcal{S}$  that we associate with input arrival times. A PPP is said to be homogeneous for constant  $\lambda(t) = \lambda$  and inhomogeneous otherwise. Example rate functions and sample realizations of the associated inhomogeneous PPP are shown in Fig. 2. These rate functions were used to generate input arrival times for the filtered shot noise process of Section 2 and the pre-synaptic spikes for the neuronal membrane of Section 6.

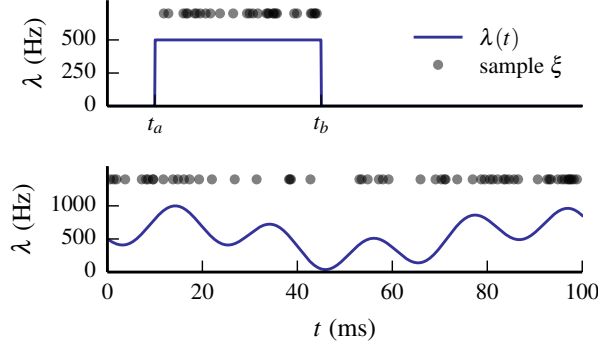


**Figure 2** – (color online) Example of rate function  $\lambda(t)$  for inhomogeneous PPP. A single realization of input arrival times  $\xi$  is represented above each rate function. The gray dots represent the location of input arrival times  $x_j \in \xi$ . (Top) Rate function used to generate input arrival times for the filtered shot noise process of Section 2. (Bottom) Rate function used to generate pre-synaptic spikes for the neuronal membrane of Section 6.

We now consider a transformation  $F(t, \xi)$  that for each real parameter  $t \in \mathcal{S}$  and realization  $\xi$  evaluates to a positive real number  $F_t = F(t, \xi)$ . The transformation is assumed invariant under permutation of  $x_j \in \xi$ , such that when written as a regular function we have  $F(t, x_1, \dots, x_n) = F(t, \{x_1, \dots, x_n\})$ .

The expectation of  $F(t, \xi)$  is obtained from the ensemble average over the number  $n$  of points and their locations  $\{x_1, \dots, x_n\}$ :

$$\langle F(t, \xi) \rangle = \sum_{n=0}^{\infty} \frac{1}{n!} e^{-m(\mathcal{S})} \int_{\mathcal{S}} \dots \int_{\mathcal{S}} F(t, x_1, \dots, x_n) \prod_{j=1}^n \lambda(x_j) dx_j \quad (5)$$

We now focus on the class of PPP transformations that are causal in the time parameter  $t$ . Such transformations ensure that arrivals  $x_j \in \xi$  later than  $t$  cannot affect the value of  $F(t, \xi)$ . In consequence, a single realization  $\xi$  generates the entire time course of  $F(t, \xi)$ . We therefore associate a *slave stochastic process*  $F_t \equiv F(t, \xi)$  to the causal PPP transformation  $F(t, \xi)$ . By construction, the expectation of  $F_t$  is the expectation of  $F(t, \xi)$  given by Eq. (5). This is illustrated in Fig. 3, where the value of shot noise process  $F_t$  at different times is evaluated from the same realization  $\xi$ .

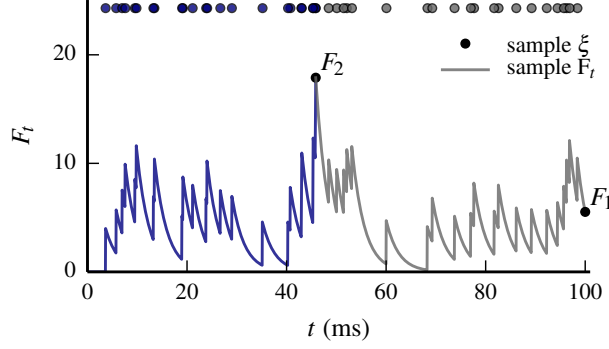


**Figure 3** – (color online) A shot noise process  $F_t$  is a causal PPP transformation  $F(t, \xi)$  of input arrival times  $x_j \in \xi$ . This particular PPP transformation is defined in Eq. (2) and its causality ensures that  $F_t$  is not affected by input arrivals later than  $t$ . For example, the value of  $F_2 = F(t_2, \xi)$  is determined by input arrivals  $x_j \in \xi$  up to  $t_2$  (blue) and is not affected by input arrivals later than  $t_2$  (gray). The gray dots represent the location of input arrival times  $x_j \in \xi$ .

We'll write  $F_1, \dots, F_K$  for the values of stochastic process  $F_t$  at times  $t_1, \dots, t_K$ ,  $\langle F_1 \dots F_K \rangle$  for its joint moments and  $\langle\langle F_1 \dots F_K \rangle\rangle$  for its joint cumulants. The expectation of PPP transformations enables to obtain analytical expressions for the joint moments and joint cumulants of  $F_t$ : its joint moments are obtained by evaluating the expectation of suitable products  $F(t_1, \xi) \dots F(t_K, \xi)$  and its joint cumulants can be constructed explicitly from the joint moments. For example, the moment  $\langle F_1 F_2^2 \rangle$  is evaluated by the expectation  $\langle F(t_1, \xi) F(t_2, \xi)^2 \rangle$ .

The causality of  $F(t, \xi)$  enables to consider the PPP in entire real line ( $\mathcal{S} = \mathbb{R}$ ) and finite activity intervals are constructed by setting  $\lambda(t) = 0$  outside finite activity windows. This approach yields exact analytical expressions for the joint cumulants of non-stationary processes generated from causal PPP transformations as will be illustrated with the non-stationary shot noise process from Section 2. A shot noise process is a particular type of *random sum*, which is a PPP transformation that factors as  $F(t, \xi) = \sum_{x_j \in \xi} f(t, x_j)$ . The joint cumulants of random sums are given by the *Campbell Theorem* [9, 15] and are also derived in the Appendix A:

$$\langle\langle F_1 \dots F_K \rangle\rangle = \int_{\mathcal{S}} f(t_1, x) \dots f(t_K, x) \lambda(x) dx \quad (6)$$

where  $f(t, x)$  is the impulse response function at time  $t$  for an input arrival time  $x$ . Shot noise is a causal random sum with  $f(t, x) = g(t - x) H(t - x)$ .

The expectation of more general forms of random sums, such as those in Eq. (3), are provided by the *Slivnyak-Mecke Theorem* [17, 18]. A comparison between numerical simulations and *Campbell Theorem* predictions are shown in Fig. 4 with excellent agreement for the mean and second order cumulants. The correlation coefficient at times  $t_1$  and  $t_2$  is given by  $\rho(F_1 F_2) = \langle\langle F_1 F_2 \rangle\rangle / (\sigma(F_1) \sigma(F_2))$  where  $\langle\langle F_1 F_2 \rangle\rangle$  is the autocorrelation at times  $t_1$  and  $t_2$  and  $\sigma(F_t)$  is the standard deviation at time  $t$ .

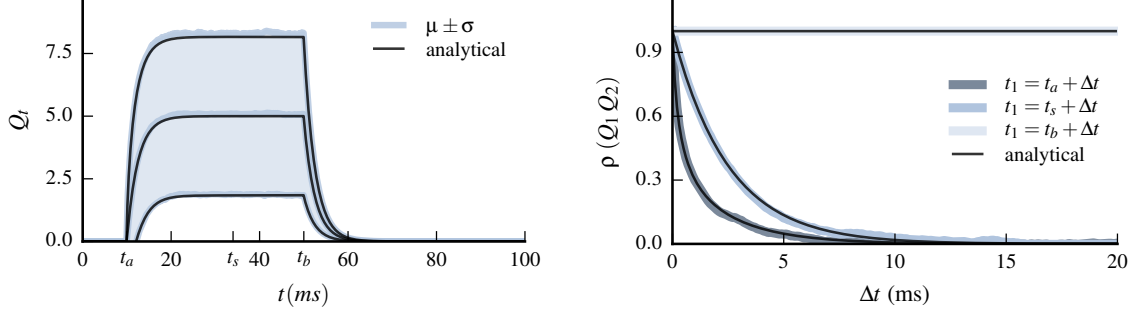


**Figure 4** – (color online) Comparison with numerical simulations for the mean and second order cumulants of shot noise process  $Q_t$  from Section 2 that are predicted by the Campbell Theorem (Eq. (6)). There is excellent agreement between the simulations (blue) and the analytic prediction (black). The correlation coefficient  $\rho$  is evaluated at  $t_a$ ,  $t_s$  and  $t_b$  corresponding respectively to the onset of PPP activity, quasi-stationary regime and the end of PPP activity.

## 4 Exact Analytical Solution

We use the properties of PPP transformations to derive exact analytical expressions for the cumulants of filtered shot noise processes with multiplicative noise and variable input rate. We investigate transformations that are relevant to these filtered processes: integral transform and random products. We evaluate their cumulants and compare with numerical simulations the predicted mean and second order cumulants of the filtered process.

According to Eq. (4), the filtered process  $Y_t$  is the integral of a causal PPP transformation that factors as a product of exponentials of input arrival times  $x_j \in \xi$ . We now investigate these transformations and define an *integral transform* of  $F(t, \xi)$  with regards to a positive and bounded function  $w$ :

$$SF(t, \xi) = \int_{-\infty}^t F(u, \xi) w(u, t) du \quad (7)$$

The mean and joint moments of the integral transform are calculated by interchanging the infinite sum and integrals of the expectation Eq. (5) with the integral of the transform. This is a consequence of the *Fubini-Tonelli Theorem* that requires either side of the equalities to exist.

$$\langle SF_t \rangle = \left\langle \int_{-\infty}^t F(u, \xi) w(u, t) du \right\rangle = \int_{-\infty}^t \langle F(u, \xi) \rangle w(u, t) du \quad (8)$$

$$\langle SF_1 \cdots SF_K \rangle = \int_{-\infty}^{t_1} \cdots \int_{-\infty}^{t_K} \langle F(u_1, \xi) \cdots F(u_K, \xi) \rangle \prod_{l=1}^K w(u_l, t_l) du_l \quad (9)$$

The linearity of integration extends Eq. (9) to the joint cumulants:

$$\langle\langle SF_1 \cdots SF_K \rangle\rangle = \int_{-\infty}^{t_1} \cdots \int_{-\infty}^{t_K} \langle\langle F(u_1, \xi) \cdots F(u_K, \xi) \rangle\rangle \prod_{l=1}^K w(u_l, t_l) du_l \quad (10)$$

We now analyze *random products* that are PPP transformations that factor as  $F(t, \xi) = \prod_{x_j \in \xi} f(t, x_j)$ . The joint moments of random products are well known, and as shown in the Appendix A:

$$\langle F_1 \cdots F_K \rangle = \exp \left( \int_{\mathcal{S}} \left( \prod_{k=1}^K f(t_k, x) - 1 \right) \lambda(x) dx \right) \quad (11)$$

We have gathered all the elements to derive the mean and joint cumulants of the filtered process  $Y_t$ . Writing  $Q(t, \xi) = Q(t)$  and using the properties of joint cumulants,

$$\langle Y_t \rangle = 1 - \frac{1}{\tau} \int_{-\infty}^t \left\langle e^{-\frac{1}{\tau} \int_z^t Q(u) du} \right\rangle e^{-\frac{t-z}{\tau}} dz \quad (12)$$

$$\langle\langle Y_1 \cdots Y_K \rangle\rangle = \left(-\frac{1}{\tau}\right)^K \int_{-\infty}^{t_1} \cdots \int_{-\infty}^{t_K} \left\langle \left\langle \prod_{k=1}^K e^{-\frac{1}{\tau} \int_{z_k}^{t_k} Q(u) du} \right\rangle \right\rangle \prod_{l=1}^K e^{-\frac{t_l - z_l}{\tau}} dz_l \quad (13)$$

The expectation of the random product of exponentials is given by Eq. (11):

$$\left\langle \prod_{k=1}^K e^{-\frac{1}{\tau} \int_{z_k}^{t_k} Q(u) du} \right\rangle = \exp \left( \int_{\mathcal{S}} \left( \prod_{k=1}^K e^{-\frac{1}{\tau} \int_{z_k}^{t_k} g(u-x) H(u-x) du} - 1 \right) \lambda(x) dx \right) \quad (14)$$

Replacing Eq. (14) into Eqs. (12) and (13) yields the exact solution for the joint cumulants of filtered shot noise process with multiplicative noise and variable input rate. The random product expectation in Eq. (14) is the key element in the evaluation of the mean and joint cumulants, which was already identified in previous work [3, 4]. As our derivation shows, this extends to any shot noise kernel  $g(t-x)H(t-x)$  and variable input rate  $\lambda(t)$  and is the main original contribution of this work.

The comparison between numerical simulations and the predictions from Eqs. (12) and (13) are shown in Fig. 5. There is excellent agreement even in such non-stationary scenario with the system undergoing transient evolution. The numerical evaluation of Eqs. (12) and (13) can be performed very efficiently with the trapezoidal rule due to the double exponential in the integrand.

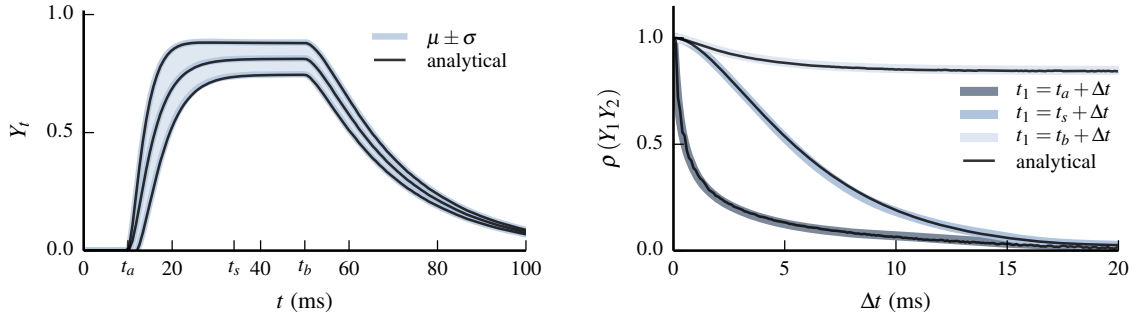


**Figure 5** – (color online) Comparison with numerical simulations for the mean and second order cumulants of filtered process  $Y_t$  predicted by the exact analytic solution given by Eqs. (12) and (13). There is excellent agreement between the simulations (blue) and the analytic prediction (black). The correlation coefficient  $\rho$  is evaluated at  $t_a$ ,  $t_s$  and  $t_b$  corresponding respectively to the onset of PPP activity, quasi-stationary  $Y_t$  and extinction of PPP activity.

The expectation of the product of exponentials (14) has a closed expression under homogeneous PPP for exponential kernel shot noise [3, 4].

## 5 Central Moments Expansion

We propose a novel approximation of the exact analytical solution that is based on a power expansion from the deterministic solution and yields a series in the central moments of integrated shot noise. We compare this approximation for the mean and second order cumulants with numerical simulations, including the case of constant Poisson rate.

The deterministic solution of Eq. (1) with mean shot noise input  $\langle Q(u) \rangle$  is given by:

$$\langle Y_t \rangle_0 = 1 - \frac{1}{\tau} \int_{-\infty}^t e^{-\frac{t-z}{\tau}} e^{-\frac{1}{\tau} \int_z^t \langle Q(u) \rangle du} dz$$

This suggests an expansion from deterministic solution  $\langle Y_t \rangle_0$  by performing a power expansion of the random product expectation in Eqs. (12) and (13). The integrated mean shot noise is first subtracted from the random product and a power expansion of the resulting exponential is performed. This corresponds to the delta method technique [19, 20] for approximating expectations of random variable transformations and yields a series in the central moments of integrated shot noise:

$$\left\langle e^{-\frac{1}{\tau} \int_z^t Q(u) du} \right\rangle \simeq e^{-\frac{1}{\tau} \int_z^t \langle Q(u) \rangle du} \left( 1 + \frac{1}{2} \left\langle \left( -\frac{1}{\tau} \int_z^t (Q(u) - \langle Q(u) \rangle) du \right)^2 \right\rangle \right)$$

This provides the following approximation for the mean of the filtered process:

$$\langle Y_t \rangle_2 = 1 - \frac{1}{\tau} \int_{-\infty}^t e^{-\frac{1}{\tau} \int_z^t (1 + \langle Q(u) \rangle) du} \left( 1 + \frac{1}{2\tau^2} \int_z^t \int_z^t \langle \langle Q(u_1) Q(u_2) \rangle \rangle du_1 du_2 \right) dz \quad (15)$$

Extending to joint moments is straightforward by expanding each exponential individually and collecting terms of the same order of  $1/\tau$ . The first order of the expansion for the autocovariance is given by:

$$\langle \langle Y_1 Y_2 \rangle \rangle_2 = \frac{1}{\tau^4} \int_{-\infty}^{t_1} \int_{-\infty}^{t_2} e^{-\frac{1}{\tau} \int_{z_1}^{t_1} (1 + \langle Q(u) \rangle) du - \frac{1}{\tau} \int_{z_2}^{t_2} (1 + \langle Q(v) \rangle) dv} \int_{z_1}^{t_1} \int_{z_2}^{t_2} \langle \langle Q(u_1) Q(u_2) \rangle \rangle du_1 du_2 dz_1 dz_2 \quad (16)$$

The comparison between numerical simulations and the predictions from Eqs. (15) and (16) are shown in Fig. 6. There is a good agreement in the transient regimes near the onset and end of PPP activity (to the right of  $t_a$  and  $t_b$ ). However, in the stationary regime (near  $t_s$ ) the second order of the expansion may be required.

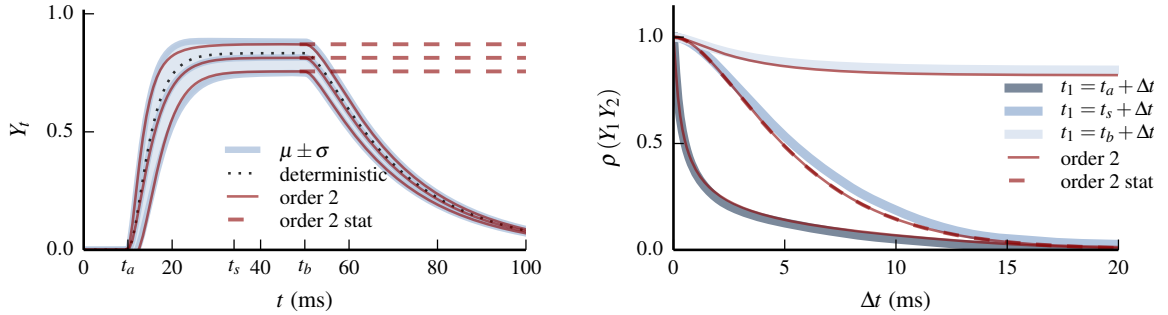


**Figure 6** – (color online) Comparison with numerical simulations for the mean and second order cumulants of filtered process  $Y_t$  predicted by the second order of the central moments expansion given by Eqs. (15) and (16). The agreement between the simulations (blue) and the analytic prediction (red) is quite good in transient regimes (to the right of  $t_a$  and  $t_b$ ) but higher order terms may be required in the stationary regime (near  $t_s$ ). The stationary limit of the approximation (red dash) and the deterministic mean (black dots) are also shown.

We found that the second order expansion for the mean and autocovariance consistently provided good results in the parameter regimes of neuron cells. Under these conditions, third and fourth order expansions either do not provide significant improvements over the second order or may even result in worse approximations. This is the case under high intensity shot noise input where much higher order terms would be needed to improve on the second order. The second order expansion for the autocorrelation is provided in the Appendix B.1 and successfully corrects the underestimated variance seen in Fig. 6.

The stationary limit of the filtered process reflects the statistics of long running trials under shot noise input with constant rate. The cumulants for this regime can be obtained by placing the onset of input arrival times at  $-\infty$  and replacing the mean and second order cumulants of shot noise in Eqs (15) and (16) with their



stationary limits. After integration by parts,

$$\langle Y_t \rangle_2 = \frac{\langle Q \rangle}{1 + \langle Q \rangle} - \frac{\langle \langle Q^2 \rangle \rangle}{(1 + \langle Q \rangle)^2} \frac{1}{\tau} \int_{-\infty}^t e^{-\frac{t-z}{\tau}(1+\langle Q \rangle)} r(t-z) dz \quad (17)$$

$$\langle \langle Y_1 Y_2 \rangle \rangle_2 = \frac{\langle \langle Q^2 \rangle \rangle}{(1 + \langle Q \rangle)^2} \frac{1}{\tau^2} \int_{-\infty}^{t_1} \int_{-\infty}^{t_2} e^{-\frac{t_1-z_1+t_2-z_2}{\tau}(1+\langle Q \rangle)} r(|z_1 - z_2|) dz_1 dz_2 \quad (18)$$

where  $\langle Q \rangle$ ,  $\langle \langle Q^2 \rangle \rangle$  and  $\langle \langle Q_1 Q_2 \rangle \rangle_{stat} = \langle \langle Q^2 \rangle \rangle r(|t_1 - t_2|)$  are respectively the mean, variance and autocovariance of stationary shot noise.

The stationary limits for the mean and second order cumulants for the exponential and alpha kernels are presented in the Appendix B.1.

## 6 Application to Neuronal Membranes

We apply the previous results to a simple model of membrane potential  $V_m(t)$  fluctuations and explore several practical and novel applications. We first calculate the non-stationary cumulants and compare them with numerical simulations. The first- and second-order central moment expansions are compared with previously published analytical estimates for the stationary limit of  $V_m(t)$ . The non-stationary cumulants are integrated in truncated Edgeworth series to approximate the time-evolving distribution of  $V_m(t)$ , and compare them with numerical simulations. We propose a simple method to estimate  $\lambda(t)$  from a small number of noisy realizations of  $V_m(t)$  and compare the inferred rate to the original pre-synaptic rate function.

We consider a simple model of the membrane potential  $V_m(t)$  for a passive neuron without spiking mechanism that is driven by shot noise conductance  $G(t)$ . This model has a single synapse type and is directly applicable to experiments where one type of synapse is isolated [21]. The time evolution of  $V_m(t)$  under conductance shot noise input  $G(t)$  is given by the following membrane equation:

$$\tau_m \frac{d}{dt} V_m(t) = E_l - V_m(t) + (E_s - V_m(t)) \frac{1}{g_l} G(t) \quad (19)$$

$$G(t) = \sum_{x_j \in \xi} g(t - x_j) H(t - x_j) \quad (20)$$

where  $\tau_m$  is the membrane time constant,  $E_l$  is the resting potential,  $E_s$  is the synaptic reversal potential and  $g_l$  is the leak conductance and  $\xi$  is a set of pre-synaptic spike times.

One realization of conductance shot noise input  $G_t \equiv G(t, \xi)$  and the resulting membrane potential response  $V_t \equiv V_m(t, \xi)$  are shown in Fig. 7, where mean and standard deviation of both processes are also represented. The numerical simulations were generated with alpha shot noise kernel  $f(t, x) = h(t - x/\tau_s) \exp(-(t - x)/\tau_s) H(t - x)$  and the rate function  $\lambda(t)$  represented in the lower plot of Fig. 2. Other parameters are  $\tau_m = 0.02$  s,  $E_l = -60$  mV,  $E_s = 0$  mV, in addition to those detailed in Section 2.

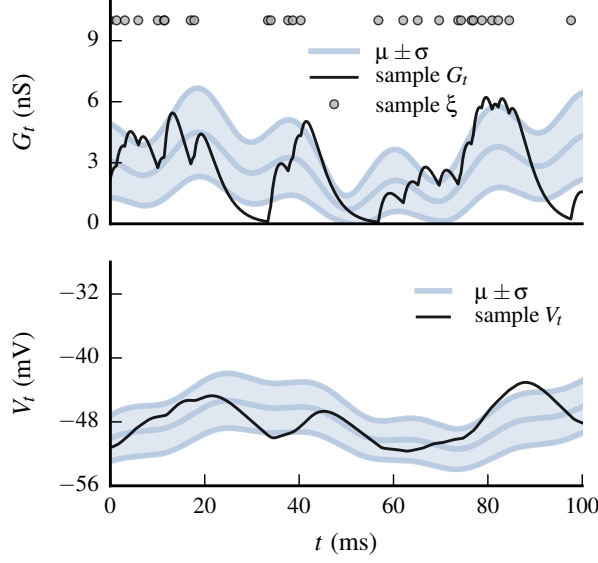


**Figure 7** – (color online) Single realization and basic statistics of membrane potential  $V_t$  fluctuations under conductance shot noise input  $G_t$ . (Top) Random pre-synaptic spike times  $x_j \in \xi$  generate non-stationary shot noise conductance  $G_t \equiv G(t, \xi)$ . The pre-synaptic spike times are distributed with a continuously varying rate  $\lambda(t)$ . (Bottom) Non-stationary membrane potential  $V_t \equiv V(t, \xi)$  driven by shot noise conductance  $G_t$ . A single realization of spike times  $\xi$  is represented by gray dots (top), realizations of  $G_t$  and  $V_t$  are shown in black. The mean and standard deviation ( $\mu \pm \sigma$ ) of  $G_t$  and  $V_t$  are shown in blue. The simulation parameters are detailed at the end of this section.

## 6.1 Non-stationary Cumulants

A first application of this formalism is to derive the mean and joint cumulants of  $V_t$  from those of  $Y_t$ . The membrane equation Eq. (19) is a scaled and translated version of Eq. (1) with the following change of variables:

$$V_m(t) = (E_s - E_l) Y(t) + E_l \quad Q(t) = \frac{1}{g_l} G(t)$$

Applying the properties of the mean and cumulants of random variables for each value of  $t$  yields the required relationships:

$$\langle V_t \rangle = (E_s - E_l) \langle Y_t \rangle + E_l \quad \langle \langle V_1 \cdots V_K \rangle \rangle = (E_s - E_l)^K \langle \langle Y_1 \cdots Y_K \rangle \rangle \quad (21)$$

The comparison between numerical simulations and the predictions from Eq. (21) are shown in Fig. 8. There is excellent agreement with the predictions from the second order of the central moments expansion given by Eqs (15) and (16), and as expected, with the exact analytical solution given by Eqs. (12) and (13). The deterministic solution is obtained from Eq. (21) by replacing  $\langle Y_t \rangle$  with  $\langle Y_t \rangle_0$  and also displays good agreement with the mean membrane potential.

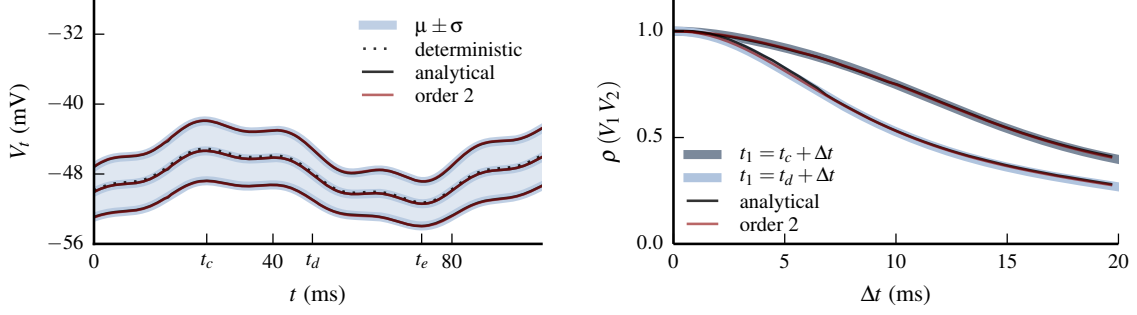


**Figure 8** – (color online) Comparison with numerical simulations for the mean and second order cumulants of membrane potential  $V_t$  predicted by the exact analytical solution (black) and the second order of the central moments expansion (red). There is excellent agreement between the simulations (blue) and the analytic prediction with both methods. The deterministic solution (black dots) also displays a good agreement with the mean membrane potential. The correlation coefficient  $\rho$  is evaluated at local maxima ( $t_c$ ) and local minima ( $t_d$ ) of  $V_t$ .

The typical mean difference between the exact analytical solution and the second order of the central moments expansion shown in Fig. 8 is in the order of 0.01 mV. Additional terms of the expansion may be required to reach similar precision in other parameter regimes. In order to illustrate this, we have increased the quantal conductance  $h$  by a factor of 20 with the effect of raising  $\langle V_t \rangle$  very close to the reversal potential  $E_s$ . As shown in Fig. 9, the second order of the central moments expansion is still in very good agreement for the mean, with an approximation error in the order of 1 mV for the standard deviation. The approximation error for the deterministic solution increases to several millivolts.

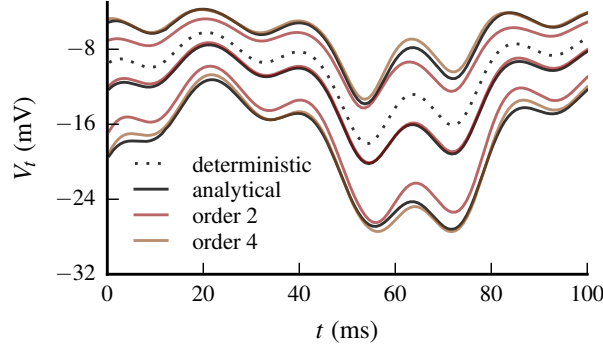


**Figure 9** – (color online) Same parameter regime as the left plot of Fig. 8 but with quantal conductance increased by a factor of 20 ( $h = 80$  nS). The mean and standard deviation of the simulated data displays excellent agreement with the analytical solution (black) but have been omitted from this figure for clarity. The approximation error for the second order of the central moments expansion (red) remain low for the mean but greatly increases for the standard deviation. The second order of the expansion for the standard deviation (brown) displays much lower approximation error but requires the evaluation of fourth order cumulants. The approximation error for the deterministic solution (black dots) greatly increases in this regime.

The Appendix B.2 provides analytical expressions for the second order of the central moments expansion in the stationary limit of  $V_t$  for the mean and autocovariance of exponential and alpha kernels. These expressions are obtained by applying Eq. (21) to Eqs. (17) and (18) and are consistent with previous analytical estimates for the mean and standard deviation that were derived with different approaches: Fokker-Planck methods for exponential kernel shot noise [22, 23] given by Eqs. (24), and a shot noise approach for alpha kernel shot noise [24] given by Eqs. (26). The analytical expressions for the autocovariance of exponential and alpha kernels are given by Eqs. (25) and (27) respectively.

## 6.2 Probability Distribution Approximation

A second application of this formalism is to use the non-stationary cumulants to approximate the time evolving distribution of membrane potential fluctuations. The mean and standard deviation of  $V_t$  yield a gaussian

approximation that is illustrated in Fig. 10. The simulations performed under the same parameters as in the left plot of Fig. 8 but with quantal conductance increased by a factor of 4 ( $h = 16$  nS). As shown in this figure, the gaussian approximation captures the time evolution of  $p(V_t)$  successfully. As expected, the skew of the distribution is not well captured by the gaussian approximation, which has been reported in both experimental [25] and theoretical studies [22, 23].

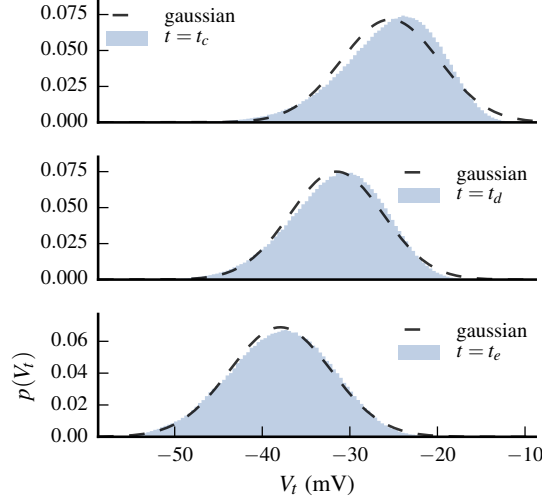


**Figure 10** – (color online) Non-stationary density of membrane potential  $p(V_t)$  evaluated at three different times:  $t_c$ ,  $t_d$  and  $t_e$  from Fig. 8. Comparison between the empirical histogram and the gaussian approximation (black slash) using the non-stationary mean and variance. The time evolution of  $p(V_t)$  is captured successfully in this approximation, which as expected also misses the skew of  $p(V_t)$ .

Deviations from the gaussian distribution are expected whenever cumulants of order three or higher are present in  $p(V_t)$ . We use a truncated Edgeworth series [19, 26, 27] to account for these deviations since it provides an asymptotic expansion of  $p(V_t)$  in terms of its cumulants. In particular, we'll use the Edgeworth series expanded from the gaussian distribution which has the advantage of coinciding with the gaussian approximation whenever cumulants of order three or higher are not present. This is an important aspect since approximately gaussian shapes of  $p(V_t)$  are sometimes present in experimental intracellular recordings. In terms of the normalized process  $X_t = (V_t - \langle V_t \rangle) / \sigma_t$  with  $\sigma_t \equiv \sqrt{\langle V_t^2 \rangle}$ , the truncated fourth order Edgeworth series is given by:

$$p_{hw}(X_t = x) \simeq \frac{1}{\sigma_t} \left( 1 + \frac{\langle V_t^3 \rangle}{\sigma_t^3} \left( \frac{x^3}{6} - \frac{x}{2} \right) + \frac{1}{4!} \frac{\langle V_t^4 \rangle}{\sigma_t^4} (x^4 - 6x^2 + 3) + \frac{10}{6!} \frac{\langle V_t^3 \rangle^2}{\sigma_t^6} (x^6 - 15x^4 + 45x^2 - 15) \right) \mathcal{N}(x) \quad (22)$$

where  $\mathcal{N}(x) = \exp(-x^2/2)/\sqrt{2\pi}$  is the standard normal density and  $p(V_t = v) = p_{hw}\left(x = \frac{v - \langle V_t \rangle}{\sigma_t}\right)$ . The third order is given by the two terms in the first line.

As illustrated by the plots on the left side of Fig. 11, the skewness of  $p(V_t)$  is indeed captured by the third order of the Edgeworth series. The bottom plot of this figure also shows a slight overestimation around the peak of  $p(V_t)$ , which it successfully captured by the fourth order term, as shown by the plots on the right side of this figure.

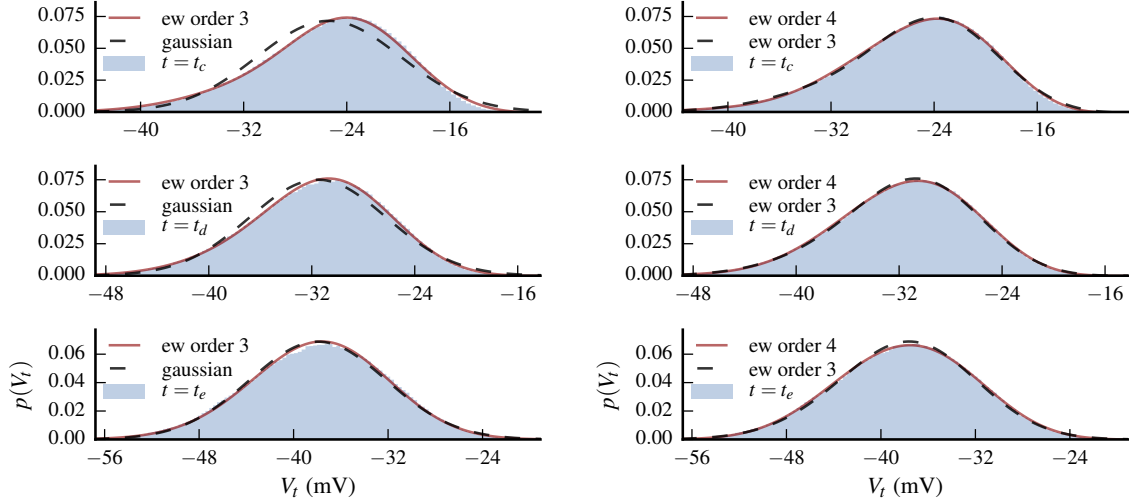


**Figure 11** – (color online) Comparison between the empirical histogram and the truncated third order Edgeworth series using the three first non-stationary cumulants (left plots). The slight discrepancy at the peak of the empirical histogram at  $t = t_e$  is captured by the fourth order Edgeworth series (right plots).

Under more extreme parameter regimes, additional terms of the Edgeworth series may be needed to capture  $p(V_t)$ . In such cases, the asymptotic character of the series becomes important since it enables to estimate the order of the truncation error that is given by the first neglected term of the series. An important caveat is that the truncated series may yield negative values for certain values of  $x$ . This is intrinsic to Edgeworth series that are constructed in the set of orthogonal polynomials associated with the base distribution (*Hermite polynomials* in the case of the standard normal distribution). The truncated series is guaranteed to integrate to unity but may result in an invalid density function since negatives values are possible. Algorithms for computing an Edgeworth series to an arbitrary order are provided in [28, 29].

### 6.3 Pre-synaptic Rate Estimation

Finally, another application of this formalism is to estimate the non-stationary pre-synaptic rate  $\lambda(t)$  from a small number  $N = 10$  of membrane potential  $V_t$  traces that are independently generated from the same PPP. Each  $V_t$  trace has a small amount of additive noise that is independent of the PPP and is sampled at rate  $1/\Delta t$ . One realization of the noisy membrane potential with mean and variance estimated from  $N = 10$  traces is shown in Fig. 12. The noisy membrane equation is given by:

$$\tau_m \frac{d}{dt} V_m(t) = E_l - V_m(t) + (E_s - V_m(t)) \frac{1}{g_l} G(t) + \epsilon(t) \quad (23)$$

where  $\epsilon(t)$  is a zero mean gaussian white noise in units of current with  $\sigma(\epsilon) = 0.2$  pA.

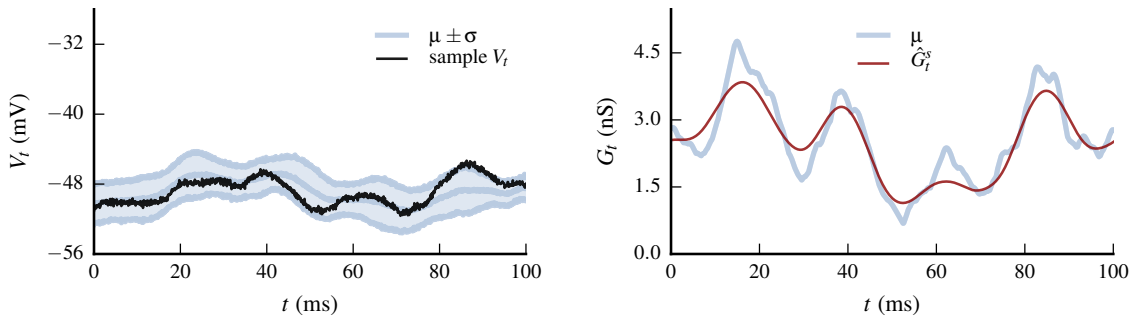


**Figure 12** – (color online) Single realization and basic statistics generated from  $N = 10$  traces of membrane potential  $V_t$  with a small amount of additive noise inherent to the instrumental measures (left plot). Smoothed version of the mean conductance input extracted from the traces of  $V_t$  using a local linear smoother with kernel bandwidth selected by cross-validation (right plot).

The key expression that enables to estimate  $\lambda(t)$  from traces of  $V_t$  is the Campbell Theorem for the mean of non-stationary shot noise given by Eq. (6). If we have knowledge of the shot noise kernel then the rate function can in principle be obtained by deconvolution of the mean conductance. However, this operation is very sensitive to noise since small changes in the estimated mean conductance will result in large changes of the estimated rate function. This aspect is dealt by filtering the estimated mean conductance prior to performing the deconvolution step. From each trace of  $V_t$  we extract the input conductance by inverting Eq. (23) and the average them to obtain the estimated mean conductance:

$$\langle \hat{G}_t \rangle = \frac{1}{N} \sum_{n=1}^N \frac{g_l}{\Delta t} \frac{\tau_m (V_{t+\Delta t}^n - V_t^n) - \Delta t (E_l - V_t^n)}{E_s - V_t^n}$$

where  $V_t^n$  is the  $n$ -th trace of  $V_t$  and  $\Delta t$  is the sampling step.

The estimated mean conductance will be a noisy version of the actual mean conductance due to the effects of the additive noise  $\epsilon(t)$  in each trace of  $V_t$ . We'll use a local linear smoother with the tricube kernel with kernel bandwidth selected by cross-validation [30]. The smoothed version of the mean conductance  $\langle \hat{G}_t^s \rangle$  is shown in the right plot of Fig. 12. Finally, we use the discrete convolution theorem to estimate the pre-synaptic rate  $\hat{\lambda}(t)$  from the smoothed mean conductance:

$$\hat{\lambda} = \frac{1}{\Delta t} \text{DFT}^{-1} \left[ \frac{\text{DFT} \left\{ \langle \hat{G}_t^s \rangle \right\}}{\text{DFT} \{g\}} \right]$$

The result is shown in Fig. 13, where the estimated  $\hat{\lambda}(t)$  rate compares favorably to the original pre-synaptic rate  $\lambda(t)$ . Estimating  $\lambda(t)$  from noisy noisy shot noise data has been addressed [31] and in particular, methods that enable to estimate the shot noise kernel in the process [32].

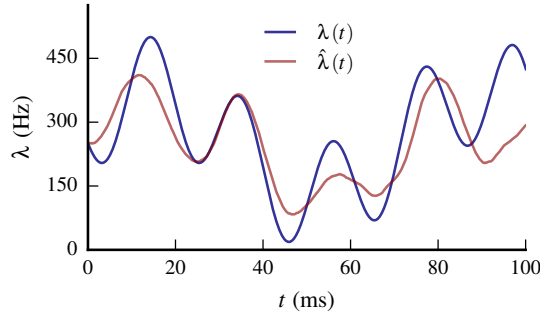


**Figure 13** – (color online) Example of estimated pre-synaptic rate  $\hat{\lambda}(t)$  (red) compared to the original PPP rate function  $\lambda(t)$ . The estimated pre-synaptic rate captures reasonably well the magnitude and variations of the original function, specially considering the small number ( $N = 10$ ) of membrane potential traces that were used for the estimation.

## 7 Discussion

In this paper, we investigated important statistical properties of filtered shot noise processes with multiplicative noise, in the general case of variable input rate. Such processes arise from the filtering of non-stationary shot noise input through a first-order ODE with variable coefficients. We have obtained general results for this class of stochastic processes, and results specific to applications to neuronal models.

We first identified the causal PPP transformation that corresponds to filtered shot noise with multiplicative noise. We investigated the statistical properties of this transformation to derive the exact analytical solution for the joint cumulants of the filtered process with variable input rate. Excellent agreement with numerical simulations was found for the mean and second order cumulants. We also proposed an approximation based on a central moments expansion from the solution of the deterministic system. We have shown with numerical simulations that the second order of this approximation is very accurate for the mean and second order cumulants.

These general results were then applied to a simple model of sub-threshold membrane potential  $V_m$  fluctuations subject to shot noise conductance with continuously variable rate of pre-synaptic spikes. Excellent agreement with numerical simulations was found for the mean and second order cumulants for both the exact analytical solution and the second order of the central moments expansion. The second order approximation for the mean and first order approximation for the variance is consistent with previously published analytical estimates for stationary  $V_m$ . An expression for the stationary limit of autocovariance is provided for exponential and alpha kernel shot noise input. An approximation for the time evolving  $V_m$  distribution is proposed that is based on a truncated Edgeworth series using the non-stationary cumulants obtained analytically. This approximation captures successfully the time evolution of  $V_m$  in all but the most extreme input rate conditions. The non-stationary mean of shot noise is used to estimate the pre-synaptic rate from a small number of intracellular  $V_m$  recordings with additive noise due to instrumental measurements.

In future work we will extend this formalism to multiple independent shot noise inputs by applying the Slivnyak-Mecke Theorem. Such development would yield direct applications for neuronal membrane models with different synapse types (such as excitatory and inhibitory synapses). Preliminary work indicates that such formalism may yield an analytic treatment of filtered shot noise with correlated input. The present work also opens perspectives for the analytical development first passage time statistics based on the non-stationary density approximations of the filtered process.

## Acknowledgments

Research supported by the CNRS, the ANR (ComplexV1 project), and the European Union (BrainScales FP7-269921 and the Human Brain Project FP7-604102). M.B. was supported by a PhD fellowship from the Marie Curie Program (FACETS-ITN FP7-237955).

## Appendix

### A Random Sums and Random Products

Random products are transformations of PPP that factor as  $F(t, \xi) = \prod_{x_j \in \xi} f(t, x_j)$ . The expectation of random products is obtained as follows:

$$\begin{aligned}\langle F_t \rangle &= \sum_{n=0}^{\infty} \frac{1}{n!} e^{-m(S)} \left( \int_S f(t, x) \lambda(x) dx \right)^n = \exp \left( \int_S (f(t, x) - 1) \lambda(x) dx \right) \\ \langle F_1 \dots F_K \rangle &= \left\langle \prod_{x_j \in \xi} \prod_{k=1}^K f(t_k, x_j) \right\rangle = \exp \left( \int_S (f(t_1, x) \dots f(t_K, x) - 1) \lambda(x) dx \right)\end{aligned}$$

In the case of the random product with  $f(t, x_j) = e^{-\frac{1}{\tau} \int_z^t g(u-x_j) H(u-x_j) du}$  and  $S = \mathbb{R}$ ,

$$\left\langle e^{-\frac{1}{\tau} \int_z^t Q(u, \xi) du} \right\rangle = \exp \left( \int_{-\infty}^z \left( e^{-\frac{1}{\tau} \int_z^t g(u-x) du} - 1 \right) \lambda(x) dx + \int_z^t \left( e^{-\frac{1}{\tau} \int_y^t g(v-y) dv} - 1 \right) \lambda(y) dy \right)$$

Random sums are transformations of PPP that factor as  $F(t, \xi) = \sum_{x_j \in \xi} f(t, x_j)$ . The joint cumulants of random sums are given by the *Campbell Theorem* [9, 15], which can be derived as follows: the *characteristic function*  $\phi(s_1, \dots, s_K)$  is the expectation of a random product and its derivatives yield the joint cumulants.

$$\begin{aligned}\phi(s_1, \dots, s_K) &\equiv \left\langle e^{is_1 F(t_1, \xi) + \dots + is_K F(t_K, \xi)} \right\rangle = \left\langle \prod_{x_j \in \xi} \prod_{k=1}^K e^{is_k f(t_k, x_j)} \right\rangle = \exp \left( \int_S \left( e^{\sum_{k=1}^K is_k f(t_k, x)} - 1 \right) \lambda(x) dx \right) \\ \langle \langle F(t_1, \xi) \dots F(t_K, \xi) \rangle \rangle &= \left( \frac{1}{i} \frac{d}{ds_1} \right) \dots \left( \frac{1}{i} \frac{d}{ds_K} \right) \ln \phi(s_1, \dots, s_K) \Big|_{s_1, \dots, s_K=0} = \int_S f(t_1, x) \dots f(t_K, x) \lambda(x) dx\end{aligned}$$

## B Central Moments Expansion

A Taylor expansion of the random product around the mean shot noise input results in a series of central moments of the integrated shot noise. Re-expressing in terms of integrated shot noise cumulants and only keeping terms of order  $(1/\tau_m)^2$ . Writing  $SQ \equiv \int_z^t Q(v, \xi) dv$  and  $S\bar{Q} \equiv \int_z^t \langle Q(u) \rangle du$ ,

$$\begin{aligned} \left\langle e^{-\frac{1}{\tau} \int_z^t Q(u, \xi) du} \right\rangle &= e^{-\frac{1}{\tau} \int_z^t \langle Q(u) \rangle du} \left( 1 + \sum_{m=2}^{+\infty} \frac{1}{m!} \left\langle \left( -\frac{1}{\tau} \int_z^t (Q(u, \xi) - \langle Q(u) \rangle) du \right)^m \right\rangle \right) \\ &\simeq e^{-\frac{1}{\tau} S\bar{Q}} \left( 1 + \frac{1}{2\tau^2} \langle\langle SQ^2 \rangle\rangle \right) \end{aligned}$$

Higher order cumulants are obtained in a similar manner by expanding each exponential individually and collecting terms in the same order of  $1/\tau_m$ . The second order expansion for the autocovariance yields:

$$\begin{aligned} &\left\langle \left\langle e^{-\frac{1}{\tau} \int_{z_1}^{t_1} Q(u_1, \xi) du_1 - \frac{1}{\tau} \int_{z_2}^{t_2} Q(u_2, \xi) du_2} \right\rangle \right\rangle \\ &= e^{-\frac{1}{\tau} S\bar{Q}_1 - \frac{1}{\tau} S\bar{Q}_2} \left( \frac{1}{\tau^2} \langle\langle SQ_1 SQ_2 \rangle\rangle - \frac{1}{2\tau^3} (\langle\langle SQ_1^2 SQ_2 \rangle\rangle + \langle\langle SQ_1 SQ_2^2 \rangle\rangle) \right. \\ &\quad + \frac{1}{2\tau^4} \left( \frac{1}{3} \langle\langle SQ_1^3 SQ_2 \rangle\rangle + \frac{1}{3} \langle\langle SQ_1 SQ_2^3 \rangle\rangle + \frac{1}{2} \langle\langle SQ_1^2 SQ_2^2 \rangle\rangle \right. \\ &\quad \left. \left. + \langle\langle SQ_1 SQ_2 \rangle\rangle (\langle\langle SQ_1^2 \rangle\rangle + \langle\langle SQ_2^2 \rangle\rangle + \langle\langle SQ_1 SQ_2 \rangle\rangle) \right) \right) \end{aligned}$$

### B.1 Stationary limit for $Y_t$

The stationary limit of shot noise autocovariance can be written  $\langle\langle Q_1 Q_2 \rangle\rangle_{stat} = \langle\langle Q^2 \rangle\rangle r(|t_1 - t_2|)$ , since:

$$\langle\langle Q_1 Q_2 \rangle\rangle_{stat} = \lambda \int_{-\infty}^{\min(t_1, t_2)} g(t_1 - x) g(t_2 - x) dx = \lambda \int_0^{+\infty} g(u) g(|t_1 - t_2| + u) du = \langle\langle Q^2 \rangle\rangle r(|t_1 - t_2|)$$

with  $r(|t_1 - t_2|) \equiv \int_0^{+\infty} g(u) g(|t_1 - t_2| + u) du / \int_0^{+\infty} g(v)^2 dv$ .

For the exponential kernel shot noise  $f(t, x) = h e^{-\frac{t-x}{\tau_s}} H(t-x)$  and  $r(|t_1, t_2|) = e^{-\frac{|t_1 - t_2|}{\tau_s}}$ . The stationary mean and second order cumulants are given by:

$$\langle Q \rangle = \lambda h \tau_s \quad \langle\langle Q_1 Q_2 \rangle\rangle = \frac{\lambda h^2 \tau_s}{2} e^{-\frac{|t_1 - t_2|}{\tau_s}} = \langle\langle Q^2 \rangle\rangle e^{-\frac{|t_1 - t_2|}{\tau_s}}$$

Writing  $Q_0 \equiv 1 + \langle Q \rangle$  and applying Eq. (17) yields the mean:

$$\langle Y_t \rangle_2 = \frac{\langle Q \rangle}{Q_0} - \frac{\langle\langle Q^2 \rangle\rangle}{Q_0^2} \frac{1}{\tau} \int_{-\infty}^t e^{-\frac{t-z}{\tau}} Q_0 \int_z^t e^{-\frac{u-z}{\tau_s}} dz = \langle Y_t \rangle_0 - \frac{\langle\langle Q^2 \rangle\rangle}{Q_0^2 \left( Q_0 + \frac{\tau}{\tau_s} \right)}$$

Applying Eq. (18) yields the autocovariance:

$$\begin{aligned} \langle\langle Y_1 Y_2 \rangle\rangle_2 &= \frac{\langle\langle Q^2 \rangle\rangle}{Q_0^2} \frac{1}{\tau^2} \int_{-\infty}^{t_1} \int_{-\infty}^{t_2} e^{-\frac{t_1 - z_1 + t_2 - z_2}{\tau}} Q_0 e^{-\frac{|z_1 - z_2|}{\tau_s}} dz_1 dz_2 \\ &= \frac{\langle\langle Q^2 \rangle\rangle}{Q_0^2 \left( Q_0 + \frac{\tau}{\tau_s} \right) \left( Q_0 - \frac{\tau}{\tau_s} \right)} \left( e^{-\frac{|t_1 - t_2|}{\tau_s}} - \frac{\tau}{\tau_s} \frac{1}{Q_0} e^{-\frac{|t_1 - t_2|}{\tau}} Q_0 \right) \end{aligned}$$

Setting  $t_1 = t_2 = t$  in the previous result yields the variance:

$$\langle\langle Y_t^2 \rangle\rangle_2 = \frac{\langle\langle Q^2 \rangle\rangle}{Q_0^3 \left( Q_0 + \frac{\tau}{\tau_s} \right)}$$



For the alpha kernel shot noise  $f(t, x) = h \frac{t-x}{\tau_s} e^{-\frac{t-x}{\tau_s}} H(t-x)$  and  $r(t_1, t_2) = e^{-\frac{|t_1-t_2|}{\tau_s}} \left(1 + \frac{|t_1-t_2|}{\tau_s}\right)$ . The stationary mean and second order cumulants are given by:

$$\langle Q \rangle = \lambda h \tau_s \quad \langle \langle Q_1 Q_2 \rangle \rangle = \frac{\lambda h^2 \tau_s}{4} e^{-\frac{|t_1-t_2|}{\tau_s}} \left(1 + \frac{|t_1-t_2|}{\tau_s}\right) = \langle \langle Q^2 \rangle \rangle e^{-\frac{|t_1-t_2|}{\tau_s}} \left(1 + \frac{|t_1-t_2|}{\tau_s}\right)$$

Proceeding as before yields:

$$\begin{aligned} \langle Y_t \rangle_2 &= \frac{\langle Q \rangle}{Q_0} - \frac{\left(Q_0 + 2 \frac{\tau}{\tau_s}\right) \langle \langle Q^2 \rangle \rangle}{Q_0^2 \left(Q_0 + \frac{\tau}{\tau_s}\right)^2} & \langle \langle Y_t^2 \rangle \rangle_2 &= \frac{\left(Q_0 + 2 \frac{\tau}{\tau_s}\right) \langle \langle Q^2 \rangle \rangle}{Q_0^3 \left(Q_0 + \frac{\tau}{\tau_s}\right)^2} \\ \langle \langle Y_1 Y_2 \rangle \rangle_2 &= \frac{\langle \langle Q^2 \rangle \rangle}{Q_0^2 \left(Q_0 + \frac{\tau}{\tau_s}\right)^2 \left(Q_0 - \frac{\tau}{\tau_s}\right)^2} \\ &\quad \left( \left( \left(1 + \frac{|t_1-t_2|}{\tau_s}\right) \left(Q_0 + \frac{\tau}{\tau_s}\right) \left(Q_0 - \frac{\tau}{\tau_s}\right) - 2 \left(\frac{\tau}{\tau_s}\right)^2 \right) e^{-\frac{|t_1-t_2|}{\tau_s}} + 2 \left(\frac{\tau}{\tau_s}\right)^3 \frac{1}{Q_0} e^{-\frac{|t_1-t_2|}{\tau_s}} Q_0 \right) \end{aligned}$$

## B.2 Stationary limit for $V_t$

We now apply the transformation given by Eq. (21) to the results from the previous section to obtain the cumulants for the membrane potential  $V_t$ . The expression for the stationary mean of the deterministic system is independent of the particular shot noise kernel and is given by:

$$\langle V_t \rangle_0 = \frac{\langle G \rangle}{G_0} (E_s - E_l) + E_l = \frac{g_l E_l + \langle G \rangle E_s}{G_0} \quad G_0 = g_l + \langle G \rangle$$

For the exponential kernel shot noise  $f(t, x) = h e^{-\frac{t-x}{\tau_s}} H(t-x)$ , the mean and variance are consistent with those given in [22, 23] and a new expression for the autocovariance is provided:

$$\langle V_t \rangle_2 = \langle V_t \rangle_0 - \frac{\langle \langle G^2 \rangle \rangle}{g_l \left(\frac{G_0}{g_l} + \frac{\tau}{\tau_s}\right) G_0} (E_s - \langle V_t \rangle_0) \quad \langle \langle V_t^2 \rangle \rangle_2 = \frac{\langle \langle G^2 \rangle \rangle}{g_l \left(\frac{G_0}{g_l} + \frac{\tau}{\tau_s}\right) G_0} (E_s - \langle V_t \rangle_0)^2 \quad (24)$$

$$\langle \langle V_1 V_2 \rangle \rangle_2 = \frac{\langle \langle G^2 \rangle \rangle}{g_l^2 \left(\frac{G_0}{g_l} + \frac{\tau}{\tau_s}\right) \left(\frac{G_0}{g_l} - \frac{\tau}{\tau_s}\right)} \left( e^{-\frac{t_1-t_2}{\tau_s}} - \frac{\tau}{\tau_s} \frac{g_l}{G_0} e^{-\frac{t_1-t_2}{\tau_s} \frac{G_0}{g_l}} \right) (E_s - \langle V_t \rangle_0)^2 \quad (25)$$

For the alpha kernel shot noise  $f(t, x) = h \frac{t-x}{\tau_s} e^{-\frac{t-x}{\tau_s}} H(t-x)$ , the mean and variance are consistent with those given in [24] and a new expression for the autocovariance is provided.

$$\langle V_t \rangle_2 = \langle V_t \rangle_0 - \frac{\left(\frac{G_0}{g_l} + 2 \frac{\tau}{\tau_s}\right) \langle \langle G^2 \rangle \rangle}{g_l \left(\frac{G_0}{g_l} + \frac{\tau}{\tau_s}\right)^2 G_0} (E_s - \langle V_t \rangle_0) \quad \langle \langle V_t^2 \rangle \rangle_2 = \frac{\left(\frac{G_0}{g_l} + 2 \frac{\tau}{\tau_s}\right) \langle \langle G^2 \rangle \rangle}{g_l \left(\frac{G_0}{g_l} + \frac{\tau}{\tau_s}\right)^2 G_0} (E_s - \langle V_t \rangle_0)^2 \quad (26)$$

$$\begin{aligned} \langle \langle Y_1 Y_2 \rangle \rangle_2 &= \frac{\langle \langle G^2 \rangle \rangle}{g_l^2 \left(\frac{G_0}{g_l} + \frac{\tau}{\tau_s}\right)^2 \left(\frac{G_0}{g_l} - \frac{\tau}{\tau_s}\right)^2} (E_s - \langle V_t \rangle_0)^2 \\ &\quad \left( \left( \left(1 + \frac{t_1-t_2}{\tau_s}\right) \left(\frac{G_0}{g_l} + \frac{\tau}{\tau_s}\right) \left(\frac{G_0}{g_l} - \frac{\tau}{\tau_s}\right) - 2 \left(\frac{\tau}{\tau_s}\right)^2 \right) e^{-\frac{t_1-t_2}{\tau_s}} + 2 \left(\frac{\tau}{\tau_s}\right)^3 \frac{g_l}{G_0} e^{-\frac{t_1-t_2}{\tau_s} \frac{G_0}{g_l}} \right) \end{aligned} \quad (27)$$

## References

- [1] A. Verveen and L. DeFelice, Progress in biophysics and molecular biology **28**, 189 (1974).
- [2] H. C. Tuckwell, *Introduction to theoretical neurobiology: volume 2, nonlinear and stochastic theories*, Vol. 8 (Cambridge University Press, 1988).
- [3] L. Wolff and B. Lindner, Physical Review E **77**, 041913 (2008).
- [4] L. Wolff and B. Lindner, Neural Computation **22**, 94 (2010).
- [5] D. Cai, L. Tao, A. V. Rangan, D. W. McLaughlin, *et al.*, Communications in Mathematical Sciences **4**, 97 (2006).
- [6] K.-i. Amemori and S. Ishii, Neural computation **13**, 2763 (2001).
- [7] J. Moller and R. P. Waagepetersen, *Statistical inference and simulation for spatial point processes* (CRC Press, 2003).
- [8] R. L. Streit, *Poisson Point Processes: Imaging, Tracking, and Sensing* (Springer, 2010).
- [9] N. Campbell, in *Proc. Camb. Phil. Soc.*, Vol. 15 (1909) pp. 310–328.
- [10] W. Schottky, Annalen der Physik **362**, 541 (1918).
- [11] B. Picinbono, C. Bendjaballah, and J. Pouget, Journal of Mathematical Physics **11**, 2166 (1970).
- [12] M. Rousseau, JOSA **61**, 1307 (1971).
- [13] D. L. Snyder and M. I. Miller, *Random Point Processes in Time and Space* (Springer, 1991).
- [14] E. Parzen, *Stochastic processes*, Vol. 24 (SIAM, 1999).
- [15] S. Rice, Bell Systems Tech. J., Volume 24 **24**, 46 (1945).
- [16] J. Rice, Advances in Applied Probability , 553 (1977).
- [17] I. Slivnyak, Theory of Probability & Its Applications **7**, 336 (1962).
- [18] J. Mecke, Wahrscheinlichkeitstheorie **9**, 36 (1967).
- [19] H. Cramér, *Mathematical methods of statistics*, Vol. 1 (Princeton university press, 1946).
- [20] G. W. Oehlert, The American Statistician **46**, 27 (1992).
- [21] M. Okun and I. Lampl, Nature Neuroscience **11**, 535 (2008).
- [22] M. Richardson and W. Gerstner, Neural Computation **17**, 923 (2005).
- [23] M. Rudolph and A. Destexhe, Neural Computation **17**, 2301 (2005).
- [24] A. Kuhn, A. Aertsen, and S. Rotter, The Journal of Neuroscience **24**, 2345 (2004).
- [25] A. Destexhe and D. Paré, Journal of neurophysiology **81**, 1531 (1999).
- [26] F. Y. Edgeworth, Transactions of the Cambridge Philosophical Society **20**, 36 (1908).
- [27] D. L. Wallace, The Annals of Mathematical Statistics , 635 (1958).
- [28] V. Petrov, “On some polynomials occurring in probability theory (russian),” (1962).
- [29] S. Blinnikov and R. Moessner, Astronomy and Astrophysics Supplement Series **130**, 193 (1998).
- [30] L. Wasserman, *All of nonparametric statistics* (Springer Science & Business Media, 2006).
- [31] R. E. Sequeira and J. A. Gubner, Signal Processing, IEEE Transactions on **43**, 1527 (1995).
- [32] R. E. Sequeira and J. A. Gubner, Signal Processing, IEEE Transactions on **45**, 421 (1997).